7-1-2014

Analysing the spatio-temporal impacts of the 2003 and 2010 extreme heatwaves on plant productivity in Europe

A. Bastos
Universidade de Lisboa

C. M. Trigo
Universidade de Lisboa

R. M. Trigo
Universidade de Lisboa

Steven W. Running
University of Montana - Missoula, steven.running@umontana.edu

Recommended Citation

Bastos, A., Gouveia, C. M., Trigo, R. M., and Running, S. W.: Analysing the spatio-temporal impacts of the 2003 and 2010 extreme heatwaves on plant productivity in Europe, Biogeosciences, 11, 3421-3435, doi:10.5194/bg-11-3421-2014, 2014.

Biogeosciences, 11, 3421–3435, 2014
www.biogeosciences.net/11/3421/2014/
doi:10.5194/bg-11-3421-2014

Biogeosciences Open Access

Analysing the spatio-temporal impacts of the 2003 and 2010 extreme heatwaves on plant productivity in Europe

A. Bastos [1], **C. M. Gouveia**[1], **R. M. Trigo**[1], **and S. W. Running**[1,2]

[1]Instituto Dom Luiz, Faculdade de Ciências, Universidade de Lisboa, Lisbon, Portugal
[2]Numerical Terradynamic Simulation Group, University of Montana, Missoula, MT, USA

Correspondence to: A. Bastos (afbastos@fc.ul.pt)

Received: 11 September 2013 – Published in Biogeosciences Discuss.: 11 October 2013
Revised: 7 May 2014 – Accepted: 27 May 2014 – Published: 1 July 2014

Abstract. In the last decade, Europe has been stricken by two outstanding heatwaves, the 2003 event in western Europe and the 2010 episode over Russia. Both events were characterized by record-breaking temperatures and widespread socio-economic impacts, including significant increments on human mortality, decreases in crop yields and in hydroelectric production.

Previous works have shown that an extreme climatic event does not always imply an extreme response by ecosystems. This work attempts to assess how extreme was the vegetation response to the heatwaves during 2003 and 2010 in Europe, in order to quantify the impacts of the two events on carbon fluxes in plant productivity and to identify the physical drivers of the observed response.

Heatwave impacts in vegetation productivity were analysed using MODIS products from 2000 to 2011. Both 2003 and 2010 events led to marked decreases in plant productivity, well below the climatological range of variability, with carbon uptake by vegetation during August reaching negative anomalies of more than 2 standard deviations, although the 2010 event affected a much larger extent. A differentiated response in autotrophic respiration was observed, depending on land-cover types, with forests increasing respiration rates in response to the heatwaves, while in crops respiration rates decreased.

The widespread decrease in carbon uptake matched the regions where very high temperature values were also preceded by a long period of below-average precipitation, leading to strong soil moisture deficits. In the case of the 2003 heatwave, results indicate that moisture deficits coupled with high temperatures drove the extreme response of vegetation, while for the 2010 event very high temperatures appear to be the sole driver of very low productivity.

1 Introduction

Heatwaves in Europe are expected to become more frequent, intense and long lasting, mostly due to the increase in mean summer temperature and corresponding variability (Luterbacher et al., 2004; Meehl and Tebaldi, 2004; Fischer and Schär, 2010). The first decade of the 21st century in Europe was particularly prone to extremely warm events (Coumou and Rahmstorf, 2012). Besides the warm summers of 2002, 2006 and 2007, this decade registered two extreme events in magnitude, spatial extent and duration, the so-called mega-heatwaves in 2003 and 2010 (Barriopedro et al., 2011).

In 2003, Europe registered the warmest summer in 500 years, with record-breaking temperatures being reached at the daily, weekly and monthly scales in western and central Europe. In large sectors of France and the Iberian Peninsula, daily maximum temperatures were between 7.5 °C and 12.5 °C above the 1961–1990 average for several weeks (Luterbacher et al., 2004; Trigo et al., 2005; García-Herrera et al., 2010). According to several authors, this event was so extreme in central Europe that it fell completely outside the range of any extreme episodes observed before, even for stations with more than 100 years of daily data (Schär et al., 2004). In this regard, despite the intrinsic difficulties in computing robust return periods for such an event, 2003 was considered extremely rare and with a low probability of occurring again in the near future (Schär et al., 2004).

Yet in 2010, Europe was stricken by an even warmer summer, with a very large extent over western Russia, registering temperatures 4 standard deviations above the reference mean for a wide range of temporal aggregations (weekly, monthly, seasonal). Barriopedro et al. (2011) have shown that the 2010 heatwave affected a much larger extent and was

far more intense than the 2003 event, with a record-breaking area of ~ 2 million km^2 compared with ~ 1 million km^2 in central Europe in 2003. These heatwaves were responsible for a significant increase of human mortality, unusually large fires and widespread impacts in ecosystems and crop yields (Trigo et al., 2005; García-Herrera et al., 2010; Barriopedro et al., 2011).

Several works have stressed the role of land–atmosphere coupling, particularly soil-moisture feedbacks, in climate variability and extremes in Europe (Seneviratne et al., 2006; Hirschi et al., 2011). Both 2003 and 2010 heatwaves were associated with persistent anti-cyclonic conditions from late spring to summer and with precipitation deficits from late winter until August. The latter, combined with increased radiation flux during late winter and spring, contributed to a rapid reduction in soil moisture through enhanced evaporation and led to persistent drought conditions. Low precipitation and soil moisture deficits during summer amplified the high temperatures reached during the heatwaves, as the reduction in evaporation was compensated by an increase in sensible heat flux (Ferranti and Viterbo, 2006; Fischer et al., 2007; García-Herrera et al., 2010; Barriopedro et al., 2011). Furthermore, Teuling et al. (2010) has shown that different land-cover types may contribute to reinforcement or attenuation of the coupling between temperature and soil moisture through non-linear evapotranspiration responses to high temperature spells.

The enhancement in carbon uptake by ecosystems observed in past decades, particularly in Europe, has been attributed to increased atmospheric CO_2 concentration and warmer springs (Zhou et al., 2001; Nemani et al., 2003; Menzel et al., 2006; Le Quéré et al., 2009; de Jong et al., 2013). However, several studies have pointed that these effects may be offset in the future due to different mechanisms such as (a) temperature increase in other seasons (Piao et al., 2008); (b) higher temperature variability or climate extremes (Heimann and Reichstein, 2008; Zhao and Running, 2010; Schwalm et al., 2012); and (c) changes in precipitation regimes (Angert et al., 2005). For instance, Ciais et al. (2005) estimated the 2003 heatwave to have reverted the equivalent of 4 years of net carbon uptake by European ecosystems. Additionally, Gouveia et al. (2008) found a reverse response of vegetation activity to increases in temperature during spring or summer in northern Europe, while Peng et al. (2013) have stressed the asymmetric effect of changes in minimum and maximum temperatures. Given the existing feedbacks between land and atmosphere and the importance of the land CO_2 sink in the global carbon budget (Ballantyne et al., 2012), reducing uncertainties about the future behaviour of ecosystems is particularly relevant for earth system science (Meir et al., 2006; Friedlingstein and Prentice, 2010; Reichstein et al., 2013). Understanding the role of climate extremes on interannual variability of carbon uptake by vegetation is thus of great interest, particularly in Europe, where ecosystems remove 7–12 % of the corresponding anthropogenic CO_2 emissions and constitute one of the most important global CO_2 forest sinks (Janssens et al., 2003; Pan et al., 2011).

The link between climatic and ecosystem extremes is not always as straightforward to establish as is often considered within the climate community. Smith (2011) has brought attention to the fact that the extremeness of a climatic event may not always translate into an extreme ecological response (Kreyling et al., 2008; Jentsch et al., 2011). Considering these limitations Smith (2011) proposed a framework to analyse the ecological impact of a climatic extreme that requires an extreme ecosystem response to be observed and attributable to the period of the extreme climatic event. Zscheischler et al. (2013) have also stressed the importance of spatio-temporal analysis to attribute biosphere responses to extreme climatic events. Furthermore, for a single climatic extreme there may be several indirect factors affecting vegetation response. The tight physical coupling between temperature and soil moisture during heatwaves may be responsible for differentiated responses of vegetation to a particular event.

This work follows the methodology proposed by Smith (2011) and performs a comparative analysis of the 2003 and 2010 heatwaves to

(i) quantify the impact of the mega-heatwaves on plant carbon uptake

(ii) assess how exceptional the response of vegetation to both events was

(iii) identify the physical drivers of vegetation dynamics.

2 Data and methods

2.1 Vegetation activity

The work relies extensively on gross primary productivity (GPP), net primary productivity (NPP) and net photosynthesis (PsN) from the improved C5 MOD17 data sets which are derived from the MODIS-NPP algorithm (Running et al., 2004) using daily meteorological data from the NCEP/DOE II Reanalysis as described in Zhao and Running (2010) and Zhao et al. (2006). This collection is an improvement of the C4 MOD17 data as described in Zhao et al. (2005), having lower uncertainties due to corrections in the meteorological inputs, in the quality control of the input radiometric data as well as a recalibration of the biome parameters.

There has been some debate about the ability of MOD17 products to reproduce real vegetation variability patterns since GPP, NPP and PsN are computed using a model that combines both spectral observations of vegetation activity (fraction of absorbed photosynthetically active radiation, fAPAR) and climatological data (Running et al., 2004). The main critiques focus on the strong influence of temperature variations in both the respiration (Q_{10}) and the vapour pressure deficit (VPD) functions (Medlyn, 2011).

Zhao and Running (2011) have performed a sensitivity analysis of these terms, concluding that relaxing the limits of maximum daytime VPD or using lower Q_{10} would lead to unrealistic values of global NPP. Furthermore, Ahlström et al. (2012) have compared the results in Zhao and Running (2010) to NPP values computed using a bottom-up approach based on a dynamic vegetation model, finding a similar response of NPP to drought conditions. Other studies have shown that MOD17 products are able to reproduce seasonal and interannual variability across a wide variety of biomes, especially in sub-tropical to polar latitudes (Running et al., 2004; Mu et al., 2007; Schubert et al., 2012; Hasenauer et al., 2012; Frazier et al., 2013) and to capture the impact of the 2003 heatwave in Europe (Reichstein et al., 2007). Nevertheless, it is worth keeping in mind that throughout the following analysis, observed patterns in GPP, NPP and PsN correspond to partially modelled results.

For annual variability analysis, MOD17A3 annual global GPP and NPP data sets were used, while for the seasonal analysis the work relied on MOD17A2 monthly PsN and GPP data sets. PsN corresponds to the difference between GPP and maintenance respiration in leaves and fine roots. Growth and woody tissue respiration are only subtracted at the end of the year to compute annual NPP (Running et al., 2004). Thus, by computing the difference between GPP and NPP, it is possible to estimate annual autotrophic respiration (Ra) fields.

Spectral observations of the fraction of absorbed photosynthetically active radiation (fAPAR) were used to assess the robustness of the results found in GPP, NPP and PsN patterns. Thus, the C5 MOD15A2 8-day fAPAR data set, also retrieved by MODIS (Myneni et al., 2002), was extracted and monthly fAPAR composites were computed from the 8-day data.

All data sets are provided at 1 km spatial resolution and were selected for a 12 yr period spanning from 2000 to 2011, over a region covering Europe, between 34.6° N–73.5° N and 12.1° W–46.8° E. Annual GPP, NPP, Ra and monthly PsN and fAPAR anomaly fields (hereafter $\mathrm{VARIABLE_{anom}}$) were also computed as the departure from the corresponding long-term average (annual or seasonal) in the study period.

The integrated European $\mathrm{NPP_{anom}}$ time series was computed for 12 yr period, and partitioned in the time series corresponding to western (longitude $< 25°$ E) and eastern (longitude $\geq 25°$ E) European sectors.

The two regions with anomalies below $-0.2\,\mathrm{kg\,C\,m^{-2}\,yr^{-1}}$ in 2003 and 2010 correspond roughly to the centres of the highest temperature anomalies registered during the summer heatwaves in each year (García-Herrera et al., 2010; Barriopedro et al., 2011) and were accordingly selected (boxes in Fig. 1b) for the following analysis, being henceforth referred to as HW03 and HW10, respectively. HW03 covers an area of $102\,000\,\mathrm{km^2}$, while HW10 covers a much larger extent, about $660\,000\,\mathrm{km^2}$.

The analysis of the annual fields does not provide a detailed assessment of the impacts of the heatwave events, which occurred during a few summer weeks. Following Smith (2011) and Zscheischler et al. (2013), a more comprehensive spatio-temporal analysis is required in order to assess if there was in fact an extreme ecological response to this climatic extreme, the amplitude of such an extreme ecological response and, if it can be attributed to the referred heatwaves. To assess the impact of the heatwaves on the seasonal cycle the work relies on monthly PsN fields and regional values which, despite lacking growth and woody respiration terms, provide information about the seasonal behaviour of carbon uptake by plants. The PsN seasonal cycle and the corresponding cumulative values in 2003 and 2010 were compared to the corresponding statistical distribution. The departure to the median and the 10–90 % variability range provides an indication of the extremeness of vegetation activity during a given period. The respective end-of-year balances of PsN relative to the median (ΔPsN) were also computed for comparison with NPP.

2.2 Land cover and burned area

Land cover was assessed by the Global Land Cover 2000 (GLC2000) data set, provided by the Global Environment Monitoring Unit of the European Commission Joint Research Centre (http://bioval.jrc.ec.europa.eu). GLC2000 makes use of a data set of 14 months of pre-processed daily global data acquired by the VEGETATION instrument on board the SPOT 4 satellite, and information is stratified into 22 classes of land cover. GLC2000 data are provided at 1 km spatial resolution and were selected over the study region, that is from 34.6° N to 73.5° N and 12.1° W to 46.8° E. Nine main land-cover types in both regions struck by the heatwaves were selected and grouped in two major categories, forests and crops. Forests correspond to GLC2000 classes 1 to 6, in other words broad-leaved (evergreen and deciduous), needle-leaved and mixed forests. Crops correspond to GLC2000 classes 16 to 18: cultivated and crops, mosaic of cropland, and tree cover and mosaic of cropland, shrub and/or grass cover. Land-cover maps of the two selected regions were analysed, with the two regions presenting similar composition: crops constitute 50 % of HW03 and 48 % of HW10, while forests correspond to 26 % of HW03 and 37 % of HW10. To provide a more detailed picture of the differentiated response of distinct land-cover types, average and integrated anomalies of GPP, NPP, Ra and cumulative PsN were computed for each of the two main land-cover categories.

As mentioned previously, the 2010 heatwave was associated to the unusual number of large wildfires, however, GLC2000 does not provide such updated information. Therefore, burned areas in 2003 and 2010 were assessed using MODIS MCD45 Collection 5.1 burned area product, which provides the approximate day of burning at 500 m spatial resolution (Roy et al., 2005). Maps for fires occurring during

summer months (JJA) were selected over the study region and re-sampled to the coarser resolution of 1 km used for all the other MODIS-based data sets.

2.3 Climate data

As MOD17 products rely on a light-efficiency model forced with spectral observations and climate data from from the NCEP/DOE II Reanalysis (Zhao and Running, 2010), part of the response observed may depend on the climate data used. Therefore, this work relies on independent data sets from ERA-Interim Reanalysis from the European Centre for Medium-Range Weather Forecasts (ECMWF) (Dee et al., 2011) and from the Global Precipitation Climatology Centre (GPCC) (Rudolf and Schneider, 2005). The effect of changes in water availability on plant productivity relied on distinct variables from the ones used to force the MOD17 algorithm: precipitation and soil moisture data (instead of VPD) which, despite being physically correlated with VPD, allow a further verification of the robustness of the results.

Monthly fields of average temperature at 2 m (T), average snow depth (SD) and volumetric soil water (SW) at four different levels (1 to 4, 0–7 cm, 7–28 cm, 28–100 cm and 100–289 cm, as in Balsamo et al., 2009), were extracted from the ERA-Interim Reanalysis (Dee et al., 2011). Data are organized on a regular grid at 0.75° spatial resolution over a region extending from 34.5 to 75° N and −13.5° W to 48° E and were selected for the study period 2000–2011.

Precipitation data was extracted from the GPCC monitoring product which is based in near-real time rain gauge observations and provides monthly mean global precipitation (P) fields at 1° spatial resolution (Rudolf and Schneider, 2005) and data were selected on a region between 34–74° N and −12° W–47° E, between 2000 and 2011. Monthly anomaly fields were computed for each climate variable after removing the seasonal cycle, and are henceforth indicated as $\mathrm{VARIABLE}_{\mathrm{anom}}$.

To understand the relationship between the observed responses in vegetation and the climate conditions in each region, the regionally averaged climatological seasonal cycle was plotted for the pairs (PsN, T), (PsN, SW1) and (PsN, SW4) and compared to the corresponding cycle during the heatwave year. Although useful to understand the evolution of climate conditions during each year in the affected regions, the departure to the mean cycle does not provide sufficient insight about the relative contribution of each climate variable to the vegetation response. To disentangle the contribution of each variable from the extreme response by vegetation, climate conditions observed during 2003 and 2010 were compared to the ones corresponding to the best and worst 25 % percentiles of PsN. Normalized values (mean $\mu = 0$ and standard deviation $\sigma = 1$) of monthly T_{anom} and $\mathrm{SW1}_{\mathrm{anom}}$ values during 2003 and 2010 (the variables known to impact more directly vegetation activity) were calculated for each pixel, averaged over the selected regions and compared to 3-year composites of the 3 best years (high annual productivity) and the 3 worst years (low annual productivity) for each region. For the calculation of the 3 worst years, the year corresponding the the heatwave was excluded, for HW03 the high (low) productivity years are 2000/2007/2011 (2001/2004/2005) and for HW10 the high (low) productivity years are 2001/2004/2005 (2002/2009/2011).

3 Results

3.1 Annual impacts

The time series of the NPP anomaly at the European scale for the 12 yr period (Fig. 1) indicates that 2003 and 2010 correspond to remarkably low values over the period, with $\mathrm{NPP}_{\mathrm{anom}}$ of about $-100\,\mathrm{Tg\,C}$ in both years. The separate analysis of the eastern and western sectors shows that these very low NPP values at the European scale were due to strong anomalies in western Europe in 2003 and in the eastern sector in 2010, coinciding with the main regions affected by the heatwaves in each year.

$\mathrm{NPP}_{\mathrm{anom}}$ fields for the 2 years (Fig. 1b) provide a better representation of the spatial variability of such low anomalies. In 2003 widespread negative anomalies were observed throughout most of Europe, with a region over southern and central France with anomalies below $-0.2\,\mathrm{kg\,C\,m^{-2}\,yr^{-1}}$ and, in some pixels even lower than $-0.4\,\mathrm{kg\,C\,m^{-2}\,yr^{-1}}$. Positive anomalies were limited to some sectors of northern Scandinavia, the UK, Ireland and western Russia. On the contrary, in 2010 it is possible to observe a large extent in western Russia with very low anomalies (from −0.2 to $-0.4\,\mathrm{kg\,C\,m^{-2}\,yr^{-1}}$) while in most of western Europe vegetation activity was close to average or slightly higher (Iberia, the Balkans and the area around the Black Sea).

The response observed in $\mathrm{NPP}_{\mathrm{anom}}$ corresponds to the balance between $\mathrm{GPP}_{\mathrm{anom}}$ and $\mathrm{Ra}_{\mathrm{anom}}$, presented in Fig. 2. $\mathrm{GPP}_{\mathrm{anom}}$ fields in both years present very similar patterns to the ones in Fig. 1b, although anomalies are considerably lower ($< -0.4\,\mathrm{kg\,C\,m^{-2}\,yr^{-1}}$) in most of the pixels affected by the heatwaves. This implies that, in those pixels, Ra was also below normal (Fig. 2b), although in HW10 a dipole pattern is observed, with the northern region presenting increased Ra, while southern areas correspond to decreased Ra. Such conspicuous patterns point to differences in the vegetation types affected, which will be further analysed.

Results of regional average balances for HW03 and HW10 are summarized in Table 1. Overall balances of GPP in HW03 and HW10 reveal distinct responses in the two regions. Despite being very similar in absolute magnitude, NPP anomalies in HW03 correspond to reductions of about 20 % of the average annual productivity, while in HW10 NPP fell below 50 % (or less) of the average NPP. In HW03, anomalies for both GPP and Ra are negative, indicating that the decrease in photosynthetic activity was followed by a decrease

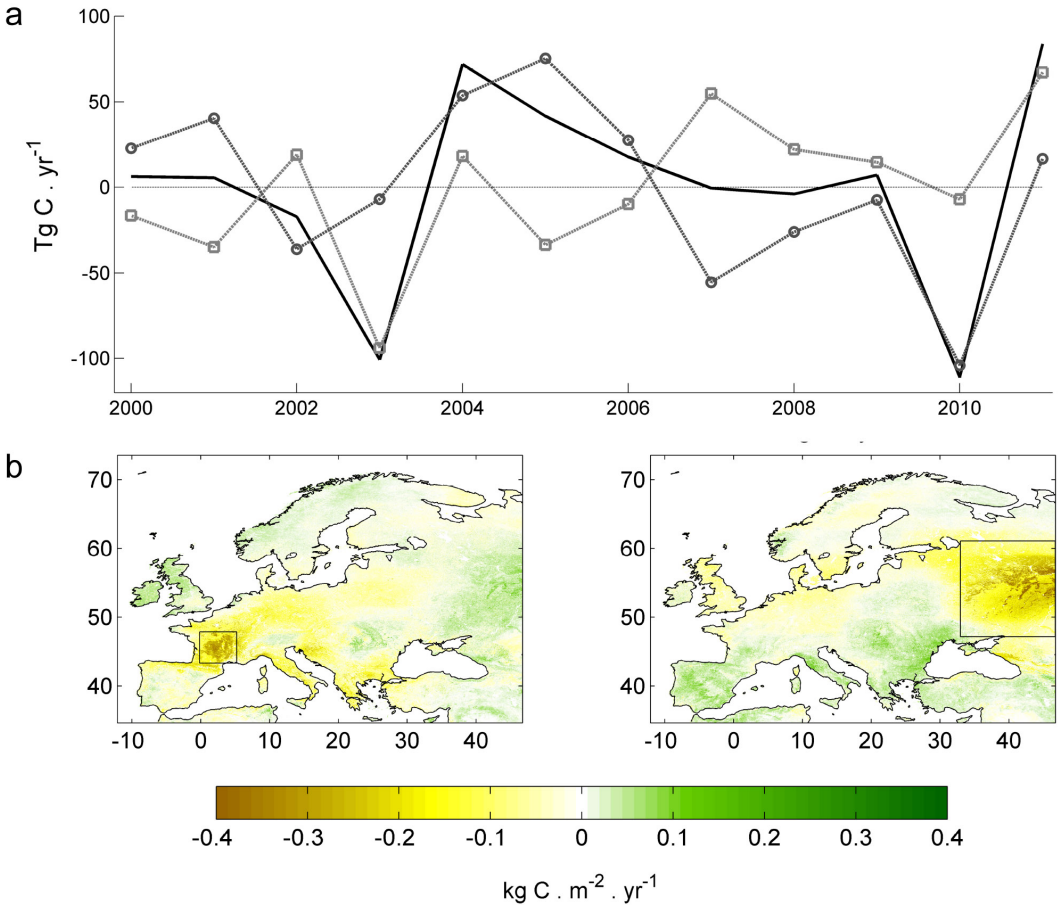

Figure 1. Annual NPP anomalies over Europe: **(a)** integrated NPP anomaly between 2000 and 2011 for Europe (solid black), western Europe (light grey dashed, circles) and eastern Europe (dark grey dashed, squares); **(b)** NPP_{anom} fields for 2003 (left) and 2010 (right). The dashed lines in **(b)** separate the western and eastern European sectors used to compute the time series in **(a)**. The reference period 2000–2011 excluding each year (2003 or 2010), to avoid the bias effect on the average of the extremely low values registered during the heatwaves. Annual NPP are derived from the MOD17A3 algorithm (Running et al., 2004) using daily meteorological data from the NCEP/DOE II Reanalysis.

in overall vegetation activity, damping the effect on NPP. On the contrary, in HW10 overall respiration presents a positive anomaly, which leads to NPP_{anom} lower than the anomaly observed in GPP. Furthermore, since the extent affected in 2010 was much larger than the one in 2003, the total NPP_{anom} resulting from the 2010 event was almost five times the value registered in the 2003 heatwave.

Results in Table 1 for the two main land-cover categories reveal an inverse response in respiration, which justify the differences observed in the regional balances. In both regions, while crops are characterized by below-average Ra values (i.e. reduced carbon release), forests present positive (i.e. enhanced carbon release) respiration anomalies. In fact, Ra_{anom} in HW10 is five times higher than in HW03 and, since forests correspond to a larger fraction of the latter region, this results in overall NPP_{anom} values below GPP_{anom} (i.e. respiration reinforces the decrease in carbon uptake). Crops present very similar values in both regions for the three variables (differences are less than $0.005\,kg\,C\,m^{-2}$), with lower magnitudes of NPP_{anom} than forests. This feature suggests higher resistance of these vegetation types to the heatwaves, however, this is most likely due to some degree of human intervention in order to minimize the impacts of the heatwave.

The analysis of the balances in burnt pixels shows that these were significant only for HW10. The widespread fires that occurred during the summer in this region primarily affected crops (68 %) and led to total NPP_{anom} values of $-1.8\,Tg\,C$, almost 2 % of the overall balance. These values reflect only the contribution of fires to the reduction in NPP observed; they do not account for the carbon emissions due to combustion or for the losses in carbon uptake over the following years before the whole ecosystem recovers, which would lead to much larger values of carbon flux anomalies.

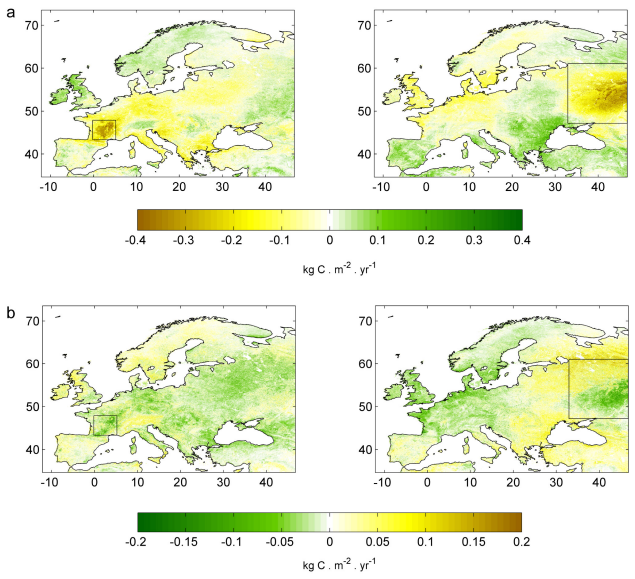

Figure 2. Annual fields of **(a)** GPP_{anom} (obtained from MOD17A3 algorithm) and **(b)** Ra_{anom} (computed as the difference between NPP and GPP) for 2003 (left) and 2010 (right) over Europe, please note the use of different scales. The colour map in Ra_{anom} is inverted so that colours match the net effect on NPP_{anom} in Fig. 1.

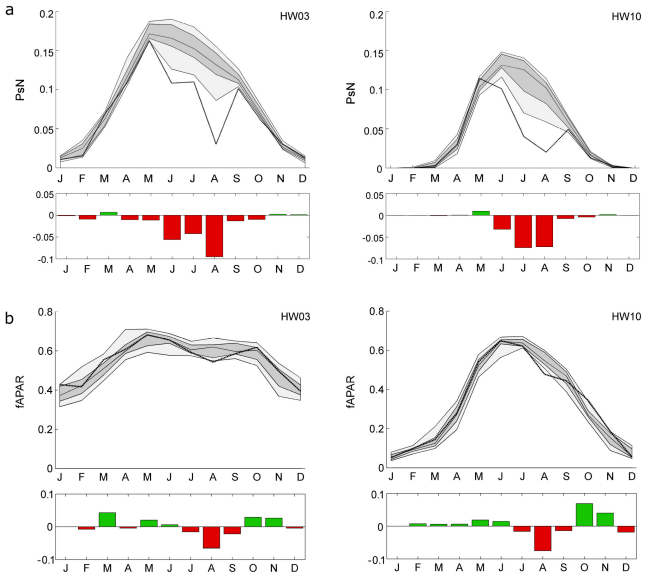

Figure 3. (a) Climatology of the seasonal cycle of monthly PsN (as obtained from MOD17A2 algorithm in $kg\,C\,m^{-2}\,month^{-1}$) for the reference period 2000–2011 averaged over the two selected regions HW03 (left) and HW10 (right). Light grey interval delimits the 10 and 90 % percentiles; dark grey delimits the 25 and 75 % percentiles; solid black line corresponds to the median. Dashed bold line corresponds to the seasonal cycle for the heatwave years, 2003 for HW03 and 2010 for HW10 and the corresponding seasonal anomalies are represented in the bottom panel. **(b)** as in **(a)** but for monthly fAPAR from MOD15A2.

3.2 Seasonal impacts

3.2.1 Seasonal cycle

The PsN seasonal cycle in 2003 and 2010 for the selected regions was compared to the corresponding climatology (Fig. 3a). Region HW03 presents a longer and more productive average seasonal cycle, reaching peak PsN values between 0.15 to 0.2 $kg\,C\,m^{-2}\,month^{-1}$, while in HW10 vegetation is generally dormant from November until March and does not reach productivity values above 0.15 $kg\,C\,m^{-2}\,month^{-1}$, explaining the differences in annual productivity mentioned previously. Moreover, PsN is characterized by larger variability in summer months, as expressed by the 10–90 % variability intervals.

During 2003, HW03 experienced lower-than-average PsN during most of the winter and spring, although still inside the 10–90 % variability range over the study period (Fig. 3a, left). From May and until October, vegetation activity was exceptionally disturbed, in particular during the summer months (JJA), when remarkably low anomalies (below $-0.05\,kg\,C\,m^{-2}\,month^{-1}$) were reached. It should be emphasized that the HW03 reached the strongest magnitude in early August 2003, however, it was preceded by an extremely warm period in June (García-Herrera et al., 2010; Barriopedro et al., 2011). In HW10, PsN remained within the 10–90 % percentiles (Fig. 3a, right) with slightly positive anomalies during the beginning of the growing season (April–May). These positive anomalies were rapidly offset during summer, especially in July and August, with PsN_{anom} values below $-0.05\,kg\,C\,m^{-2}\,month^{-1}$. It is worth noting that in both regions August was the month registering the largest departure from the 10–90 % range, coinciding with the strongest period of the heatwave events. Analysis of seasonal GPP (now shown) reveals a very similar behaviour, with anomalies below the 10 % percentile during summer months in both regions.

Analysis of monthly fAPAR (Fig. 3b) shows that before the summer months, vegetation activity was close to or even above average in both regions. In HW03 fAPAR shows very high positive anomaly in March, remaining close to average until June, while negative anomalies are already observed in PsN. In HW10 fAPAR remains above average from late winter to early summer, matching the slight enhancement in PsN in late spring, but not the strong negative PsN_{anom} value reached in June. In both regions, only during summer months (JAS) are negative fAPAR anomalies found, however these reach extreme values only in August, when fAPAR clearly stays below the 10 % percentile.

3.2.2 Carbon balance

The preceding months with above-average PsN have a positive impact on the total carbon uptake during the seasonal cycle, cancelling out part of the negative impact of the

Table 1. Relative and total GPP_{anom}, NPP_{anom}, Ra_{anom} and difference in accumulated PsN during 2003 (HW03) and 2010 (HW10) for each region. Values for forests, crops and total area are given in each column. Results are presented as average carbon uptake (in $kg\,C\,m^{-2}$) and the corresponding integrated balance over each region (in Tg C).

		Forests		Crops		Total	
		HW03	HW10	HW03	HW10	HW03	HW10
GPP_{anom}	$kg\,C\,m^{-2}$	−0.25	−0.13	−0.15	−0.15	−0.21	−0.13
	Tg C	−6.5	−30.1	−7.6	−48.9	−20.8	−90.1
NPP_{anom}	$kg\,C\,m^{-2}$	−0.25	−0.18	−0.13	−0.13	−0.19	−0.14
	Tg C	−6.7	−40.7	−6.6	−42.5	−18.9	−93.6
Ra_{anom}	$kg\,C\,m^{-2}$	0.01	0.05	−0.02	−0.02	−0.02	0.01
	Tg C	0.2	10.5	−1.0	−6.4	−1.9	−3.4
ΔPsN	$kg\,C\,m^{-2}$	−0.30	−0.24	−0.22	−0.18	−0.23	−0.19
	Tg C	−7.2	−55.1	−14.9	−56.0	−23.0	−125.0
% of area		26	37	50	48	–	–

heatwaves, and worth assessing the evolution of the cumulative carbon balance (Fig. 4a, coloured lines). The cumulative balances of PsN in both regions start to depart from the median only by the end of spring and present much lower accumulation rates during summer, especially in August. The end-of-year departure from the median is quite similar for both regions (about $0.25\,kg\,C\,m^{-2}$), however, relative to the corresponding standard deviation, the impact of the heatwave on PsN in HW10 was slightly higher, reaching $-2.8\,\sigma$ in August 2010 (Fig. 4a), while in HW03 the departure in August 2003 was $-2.4\,\sigma$ (Fig. 4a). From October to December, cumulative PsN curves for the two extreme years follow a similar trajectory as the respective climatologies, thus the negative balance is mainly due to the decrease in PsN during JJA.

Results for forests and crops (Fig. 4b and c) indicate that forests, the most productive land-cover type, were affected more severely. In HW03 forests registered null or slightly negative PsN (i.e. turning into a source of CO_2) from July to August. Again, this evolution between July and August 2003 reflects to a certain extent the double nature of the 2003 heatwave in western Europe with an early peak in June and a stronger one in August (García-Herrera et al., 2010; Barriopedro et al., 2011). Crops in general present a weaker response to the heatwaves, relative to forests. In the case of the sub-class cultivated and croplands, the departure does not even fall outside the climatological variability range. Table 1 summarizes end-of-year balances of PsN relative to the median, over the total area and discriminated for the main land-cover types. In both regions, forests suffer greater relative losses, however, crops contribute more to the area-integrated balance in HW03, while in HW10 the two main land-cover types contribute in approximately equal parts to the total balance.

3.2.3 Spatial patterns

Assessing whether the major decreases in vegetation carbon uptake during summer were a direct response to the high temperatures registered during the heatwaves requires the analysis of seasonal evolution of PsN_{anom} spatial patterns during 2003 and 2010 (Figs. 5 and 6, respectively) and further comparison with the corresponding climate patterns.

Western and central Europe experienced low levels of productivity from the early beginning of 2003 (Fig. 5). In April, very low PsN_{anom} values were observed in the Balkans, but were followed by 2 months of enhanced productivity. In June a large area of PsN anomalies below $-0.2\,kg\,C\,m^{-2}$ formed over southern and central France (the region corresponding to HW03), which remained approximately stable during July. In August, the region with very low PSN_{anom} spread over most of western and central Europe. It is worth noting the strongly enhanced productivity observed in western Russia and some sectors of Eastern Europe during the summer, especially in July and August, of 2003.

In 2010, more contrasting patterns were observed (Fig. 6). Above-average productivity in May over most of eastern Europe was then followed in June by PsN_{anom} values below $-0.2\,kg\,C\,m^{-2}$ on a very large region centred in western Russia, while throughout most of Europe high productivity was still observed. In July, the region with very low PsN_{anom} spread north-westwards, affecting some parts of Scandinavia, the UK, northern Germany and Poland. In August, the area of low PsN_{anom} values over western Russia was further enlarged southwards, while in many sectors of western and central Europe PsN was again enhanced.

3.3 Climate patterns

Figures 7 and 8 summarize results for the climatic conditions observed during spring and summer (March–September) in

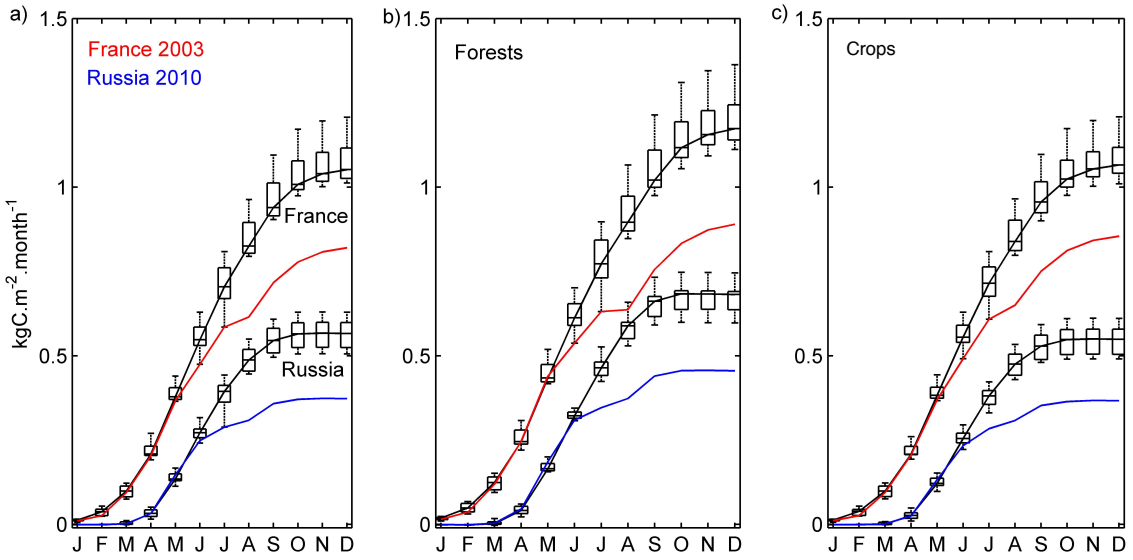

Figure 4. (a) Accumulated monthly PsN (from MOD17A2) climatology (box plots and black lines) for the two selected regions HW03 and HW10. Boxes represent the $\pm 0.5\,\sigma$ range and whiskers extend to the most extreme data that are not outliers. Accumulated monthly PsN for 2003 in region HW03 (red) and for 2010 in region HW10 (blue). **(b)** and **(c)** as in **(a)** but for forests and crops, respectively.

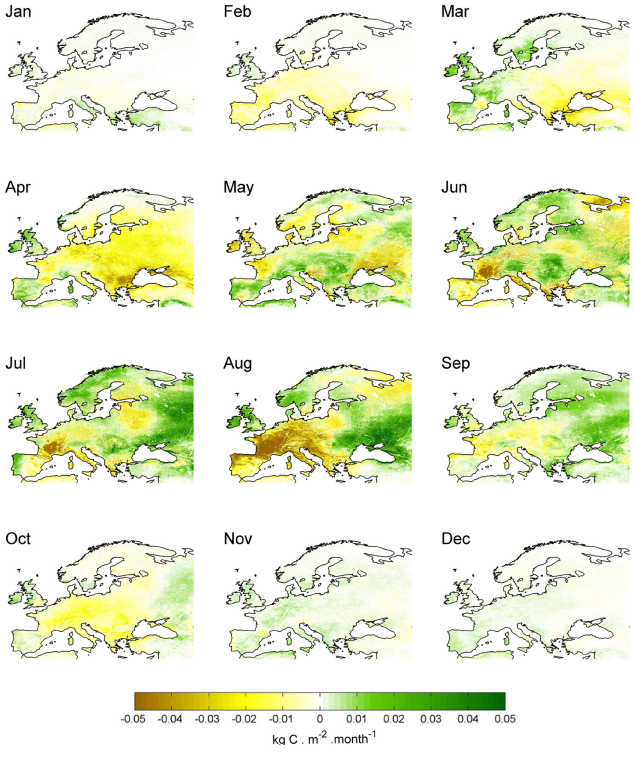

Figure 5. Monthly $\mathrm{PsN}_{\mathrm{anom}}$ fields from MOD17A2 during 2003.

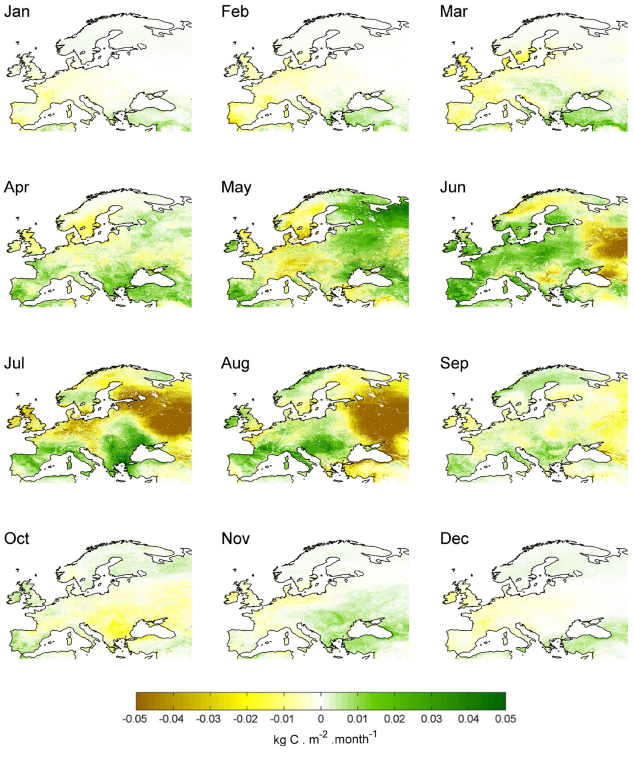

Figure 6. As in Fig. 5, but for 2010.

2003 and 2010, respectively, for T_{anom}, P_{anom}, $\mathrm{SW1}_{\mathrm{anom}}$ and $\mathrm{SW4}_{\mathrm{anom}}$.

The strong PsN anomalies (Figs. 5 and 6) match the patterns of very high temperature anomalies shown in Figs. 7a and 8a. In southern and central France, temperatures reached anomalies higher than 4 °C in June and August of the same year (Fig. 7a). However, in July 2003, temperatures in this region were only about 1 °C above average, and still very

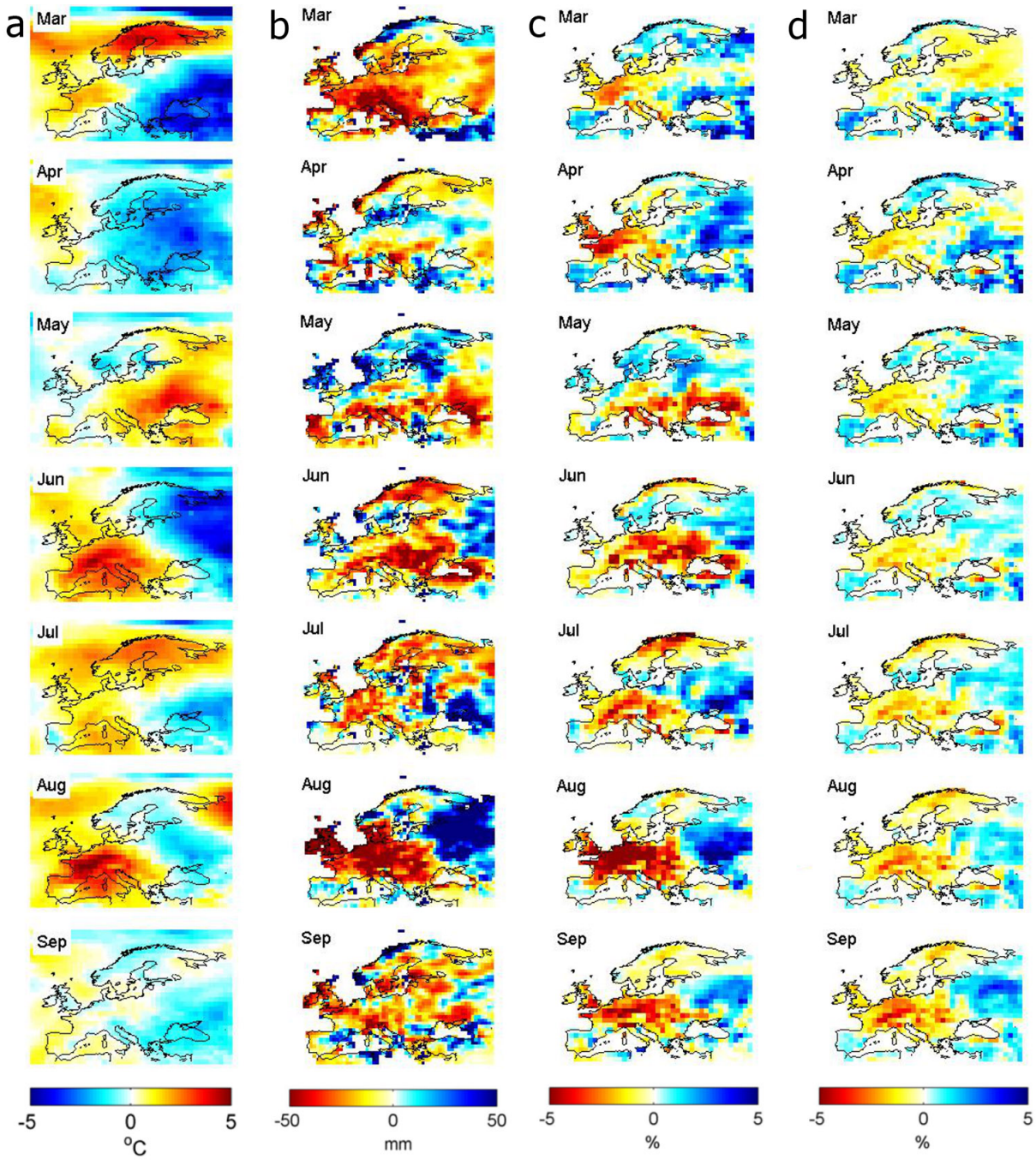

Figure 7. Monthly climate anomalies over Europe during spring and summer 2003: **(a)** average temperature at 2 m (T_{anom}); **(b)** precipitation (P_{anom}); **(c)** volumetric soil water at level 1, 0–7 cm ($SW1_{anom}$); and **(d)** volumetric soil water at level 4, 100–289 cm ($SW4_{anom}$). T_{anom}, $SW1_{anom}$ and $SW4_{anom}$ fields from the ERA-Interim Reanalysis and P_{anom} from GPCC, based in near-real time rain gauge observations.

low PsN_{anom} persisted. Strong precipitation deficits were observed (Fig. 7b) throughout most of central and western Europe in 2003, especially in early spring (March) and all the summer months, where P_{anom} values below 50 mm month^{-1} were registered. Soil moisture deficits in top and deep layers (Fig. 7c and d) were observed in central Europe during spring and summer, particularly at the top layer (SW1), but were considerably exacerbated between June and August. The dry conditions may thus explain the persistence of low PsN anomalies between the stronger heat spells.

In 2010, the moderately cool spring months (March and April) over most of Europe (Fig. 8a) were followed by

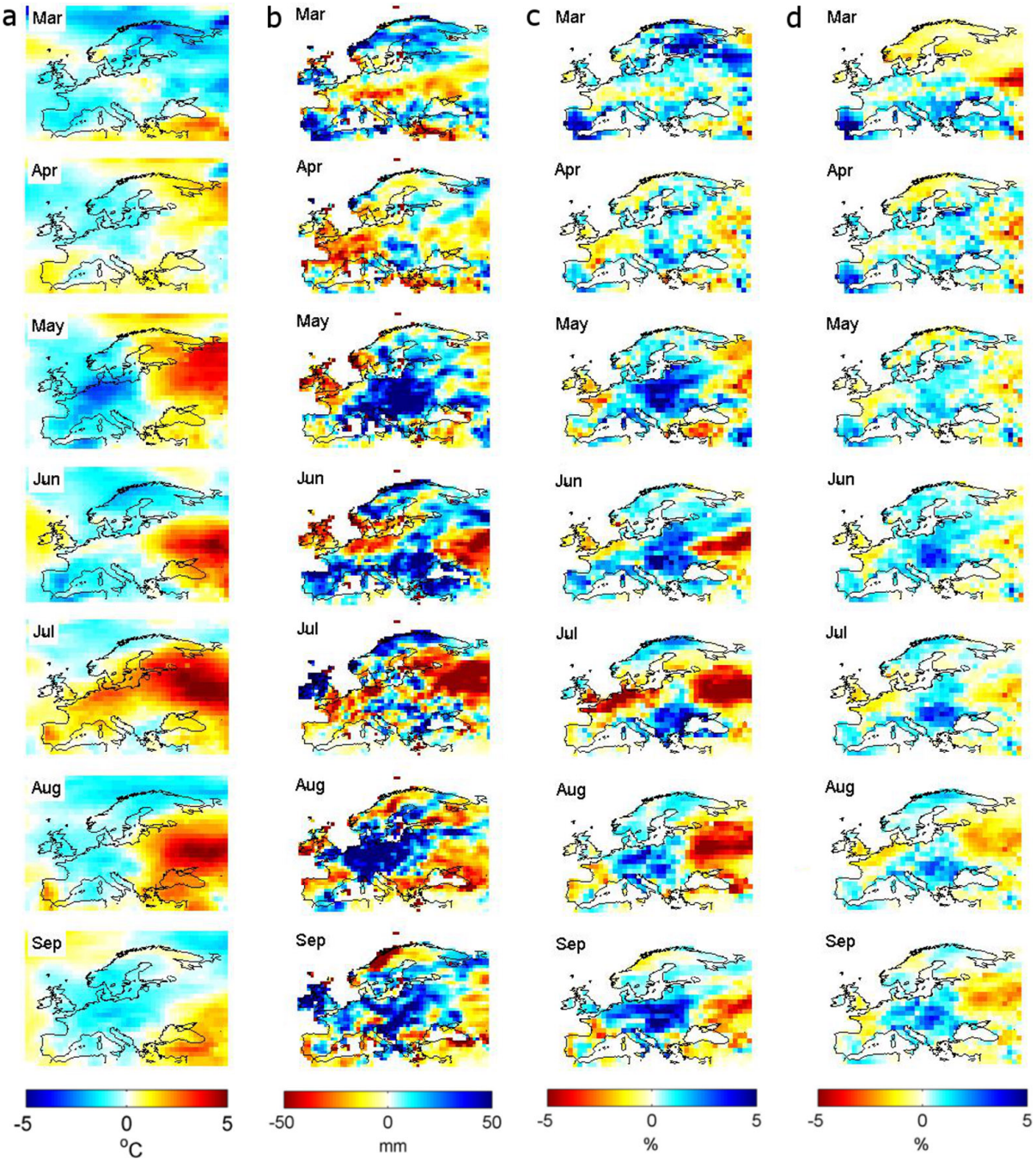

Figure 8. As in Fig. 7, but for 2010.

temperature anomalies of about 3–4 °C over western Russia, which persisted and further increased during summer months (JJA). Particularly, in a very large extent around Moscow, T_{anom} values over 5 °C persisted for 2 consecutive months (JA). Cooler-than-average temperatures were generally observed over the rest of Europe, except during July, which was warmer than average practically over all regions. Precipitation patterns (Fig. 8b) are not as clear as in the case of 2003, although small precipitation deficits appear to have prevailed during spring in western Russia. In June and July, P_{anom} values below $-50\,mm\,month^{-1}$ were observed over western Russia, northern Germany, Poland and the UK. These precipitation deficits are also reflected in SD_{anom} fields (not shown) which present negative anomalies during winter and early spring in that region. In spring 2010, soil moisture fields are characterized by different dynamics on the top and

deep layers. In March, in western Russia and Scandinavia, on the top layer (Fig. 8c) $SW1_{anom}$ values above 4 % were registered, while in the deeper layer ($SW4_{anom}$, Fig. 8d), values were 1 to 4 % lower than average. This enhancement of soil moisture on the top layer was possibly due to an earlier snowmelt in the beginning of spring (not shown), in accordance to Barriopedro et al. (2011). In the rest of spring and summer, $SW4_{anom}$ dynamics follows $SW1_{anom}$ although with attenuation and an apparent lag of about a month, with SW1 achieving a prominent negative value in July and August, while SW4 presents the (less intense) peak anomalies in August and September. Results obtained for the patterns of T, P and SW are consistent with results obtained in previous works (Ferranti and Viterbo, 2006; Fischer et al., 2007; García-Herrera et al., 2010; Barriopedro et al., 2011).

3.4 Climate drivers

Climate and vegetation conditions throughout the year are compared to the respective climatology for the two selected regions in Fig. 9. Generally, PsN increases with increasing T during winter and spring, peaking in late spring (region HW03) or early summer (region HW10). In the region HW10, the amplitude of the annual cycle of T is higher (notice different xx axis scales), and a dormant period appears clearly associated to those months with negative or very low T. Both areas are characterized by wet winters and dry summers, with soil water peaking at lower values in late summer. The region corresponding to HW10 is, in general, wetter than HW03 at both top and deep layers and presents higher seasonal variability on the annual cycle.

In HW03, the biggest departure of PsN from the climatological seasonal cycle in 2003 occurs during JJA, with increasing temperature and remarkable SW1 deficits (Fig. 9a). In September, although temperature returns to average values, PsN is still below normal, matching the reduction still observed in soil moisture at the top and deeper layers. After October, PsN returns to normal values as well as T and SW1, while in SW4 large deficits remain. The dynamics of HW10 during 2010 (Fig. 9b) is very similar to the one described for HW03, with the biggest departures of PsN from the climatological cycle being registered in summer months,especially during August, with increased temperatures and reduced soil moisture in the top layer.

The patterns suggest a differentiated response to high temperatures in distinct periods of the phenological cycle. In May 2010, very high temperature and relatively small moisture deficits (~ -1 %), are associated to an enhancement of PsN (Figs. 3 and 6) in western Russia. Since May corresponds to the beginning of the phenological cycle (Fig. 3), increased temperatures may increase photosynthesis rate (Nemani et al., 2003), provided that soil moisture deficits are not extreme. In both years, the patterns observed in PsN dynamics (Figs. 5, 6 and 9) depend crucially on the evolution of

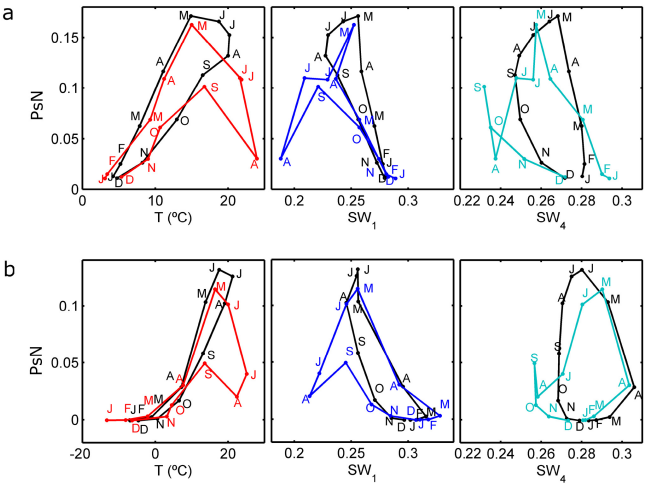

Figure 9. Climatological seasonal cycle (black lines) and seasonal cycle on the heatwave year (coloured lines) of (xx axis) T (left panel, red lines), SW1 (central panel, blue lines) and SW4 (right panel, cyan lines) from ERA-Interim versus PsN (yy axis) in kg C m^{-2} month^{-1} for **(a)** HW03, heatwave year 2003 and **(b)** HW10, heatwave year 2010.

temperature but also, to some extent, of soil moisture, particularly in the top layer (Figs. 7c, 8c and 9).

The combination of high temperature with long-term precipitation deficits increases soil moisture depletion, producing a positive feedback that further enhances the heatwave intensity, as Seneviratne et al. (2006) and Hirschi et al. (2011) have shown. To identify which variable (or variables) was responsible for the extreme ecological response, normalized monthly values of T_{anom} and $SW1_{anom}$ during 2003 and 2010 are compared with the best years (high annual productivity) and worst years (low annual productivity) composites for each region (Fig. 10).

In the case of HW03 (Fig. 10, left panel), the heatwave was associated to both temperature and soil moisture anomalies well outside the average conditions during the worst years. In HW03, the composite for the best years is associated with warm springs and cool and wet summers, while the worst years present an inverse pattern. In 2003, T_{anom} during summer months was more than 3σ above the composite for the worst years, while $SW1_{anom}$ in July and August fell below the values in worst years by more than 2σ. Highly productive years in HW10 appear associated with wet spring and summer months and moderately cool summer temperatures, with lower-than-average years mostly associated with dry conditions and average temperatures. In HW10 (Fig. 10, right panel), T_{anom} was about 3σ or more above the values for the worst years during most of the growing season, however $SW1_{anom}$ values do not appear to fall far for the variability range of that region (about $\pm 1\sigma$ or less). In fact, during May and June the values are even higher than registered in the worst years. The difference in results between the

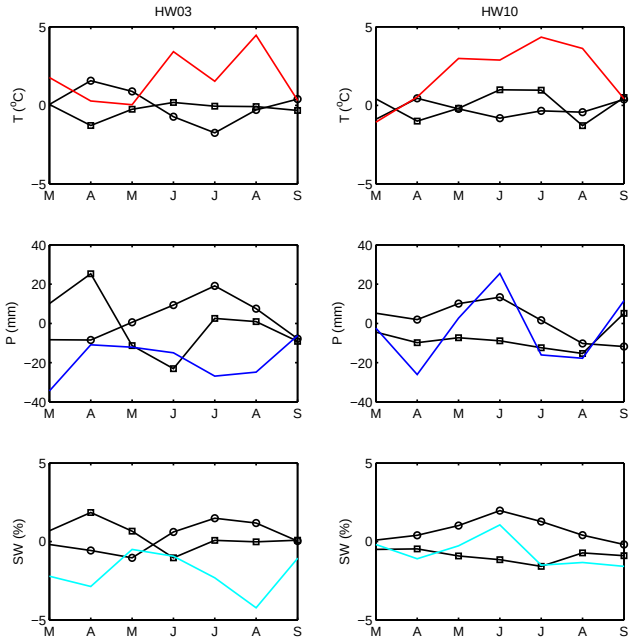

Figure 10. Normalized monthly values from March to September of **(a)** T_{anom} **(b)** P_{anom} and **(c)** $SW1_{anom}$, averaged over each region for: composites of best years (black line, circles), worst years (black line, squares), and 2003 (HW03, colour lines, left panel) or 2010 (HW10, colour lines, right panel). Units in the *yy* axis correspond to standard deviations of each variable. Worst years are computed excluding the heatwave year for each region. For HW03 the high (low) productivity years are 2000/2007/2011 (2001/2004/2005) and for HW10 the high (low) productivity years are 2001/2004/2005 (2002/2009/2011).

two regions indicates different contributions of each variable to the extreme response of vegetation during the heatwave. While in HW03, the extremely low values of plant productivity appear to be driven by a combination of high temperatures and strong soil moisture deficits; in HW10 soil moisture values, despite being lower than average, were comparable to or higher than low productivity years.

4 Discussion and conclusions

During 2003 and 2010 in Europe a marked decrease in vegetation carbon uptake was observed at the monthly, seasonal and annual scales. This work intends to assess whether these deficits were a response to the two record-breaking heatwave events that struck different regions in Europe during summer in those years, and how extreme (in a climatological sense) were the observed anomalies.

On the annual scale, NPP anomalies fell below $-0.2\,\mathrm{kg\,C\,m^{-2}\,yr^{-1}}$ in both years, although in 2010 a much larger extent with very low anomalies ($< -0.4\,\mathrm{kg\,C\,m^{-2}\,yr^{-1}}$) was affected. The anomalous values observed in NPP depend primarily on GPP anomalies but also on the contribution of Ra. In the HW03 sector, the decrease in GPP during the heatwave is accompanied by a decrease in Ra, attenuating the impact on NPP. Results are consistent with the analysis in Ciais et al. (2005), which relied on an ecosystem model to compute total ecosystem respiration and showed a drop in both autotrophic and heterotrophic respiration, together with GPP, during 2003. In region HW10, a marked difference is observed in Ra anomalies between the northern (increased Ra) and the southern sector (decreased Ra) during 2010. Such clear north–south differences in Ra (under similar climatic conditions) result from a differentiated response of vegetation to the heatwaves depending on land-cover type.

The comparison of the impact of the heatwaves on GPP, NPP and Ra between forests and crop areas reveals that the larger decrease in NPP in forests is due to increased respiration, while in crops the reduction in GPP is followed by a drop in respiration rates. This decrease, rather than an enhancement with high temperatures, indicates a stronger control of biomass production and respiration in crops than in forests. Since crops are mainly annual or sub-annual cultures, respiration is expected to depend mainly on biomass produced during the growing season, while in forests respiration depends on the total amount of biomass accumulated in the tissues of the trees during their lifetime. If, in the total balance of HW03 the latter effect is negligible because Ra_{anom} values are very small and crops dominate the region, in the case of HW10 increased autotrophic respiration in forests makes their contribution of overall NPP anomalies to be similar to that obtained for crops.

Seasonal analysis of vegetation activity in the selected regions indicates that photosynthetic activity (as given by fAPAR) and carbon uptake (PsN) close to (or above) average during spring and began to decline by late spring, with the larger drops in carbon uptake by vegetation occurring during summer months, along with extremely high temperatures. In both years, monthly PsN started to fall markedly outside the 10–90 % variability range only from June onwards, and reached larger departures (more than two standard deviations) in August. The dynamics in PsN is not completely reflected in fAPAR anomalies, which could suggest a milder impact of the heatwaves on vegetation conditions during 2003 and 2010. However Reichstein et al. (2007) have previously observed the same discrepancies between fAPAR and eddy covariance carbon flux measurements, suggesting that these differences may be due to physiological responses of vegetation to dry periods, for instance with some of the radiation absorbed being dissipated rather than used in photosynthesis. Furthermore, strong negative fAPAR anomalies are observed when leaves turn brown and wilt, a process that takes longer to occur, even if photosynthesis is already below normal. Nevertheless, in both years, fAPAR falls outside the 10–90 % range in August (coinciding with the heatwave events) which reinforces the conclusions about the outstanding impact of the heatwaves on vegetation activity.

Thus, according to the framework used in this work (Smith, 2011), only from June to August was an actual extreme ecological response observed. Both years were characterized by persistent dry conditions preceding the heatwaves, especially in the case of 2003, with precipitation below normal leading to water deficits in all soil layers, which further enhanced the temperatures reached during the heatwaves. These persistent dry conditions preceding the heatwave are particularly relevant in the case of the 2003 event, and appear to have contributed to the negative PsN anomalies observed from spring to early summer as already pointed in other works (Ciais et al., 2005; Reichstein et al., 2007). On the seasonal scale, HW03 and HW10 present similarly extreme responses (PsN more than 2 standard deviations below average), however, on the annual scale the heatwave had a stronger impact on HW10, where NPP fell more than 50 % below average, while in HW03 anomalies were ~ 20 %. The temporal coincidence of the extreme PsN and fAPAR values, with the periods of higher temperature anomalies, points to a clear impact of the heatwave event, nevertheless, it must be stressed that the heatwave may impact vegetation activity through both high temperatures and reduced soil moisture due to the feedbacks between both variables during heatwave events (Seneviratne et al., 2006).

This work attempts to disentangle the contribution of each climatic factor from the very low values of CO_2 uptake by vegetation observed as response to the heatwaves and understand whether this response was driven by the extremely high temperatures, by reduced water availability, or by a combination of both factors. The analysis of the anomaly values of T and SW during the best and worst years in terms of vegetation productivity, and the comparison with the corresponding values during the heatwave years for each region uncovers important differences between the two events and highlights the usefulness of this approach to assessing drivers of vegetation activity during extreme events. In the case of HW03, the heatwave months correspond to temperatures well above the ones registered for either the best and worst years, together with soil moisture anomalies far below the ones attained during the worst years. However, for HW10, extreme values are observed only for temperature anomalies, while soil moisture remains inside (or very close to) the best and worst years' curves. In fact, in other years when photosynthetic activity was very low (but still higher than in 2010), vegetation experienced even lower values of soil moisture. The comparison of the two events in 2003 and 2010 allows for distinguishing different behaviours: while in 2003 the observed declines in PsN suggest a strong impact of the long dry period preceding the heatwave, in 2010 extremely high temperatures appear to be the main factor leading to low PsN. In HW10, despite water deficits being observed these do not appear to be particularly extreme for vegetation, implying that the extreme response observed in HW10 was mainly driven by the very high temperature anomalies.

This work emphasizes the fact that an extreme climatic event (a heatwave) may lead to distinct responses of vegetation that may or may not be considered extreme. Responses may differ either because of the combined effect of the extreme event with other disturbance (e.g. drought) or the different ability of plants to cope with extreme climate conditions. Since heatwaves are characterized by a strong coupling between temperature and soil moisture, the driving variables of the ecological response may differ from one event to another, depending on the strength of the coupling, on vegetation type and on human factors, such as land management practices.

Acknowledgements. Ana Bastos was funded by Portuguese Foundation for Science and Technology (SFRH/BD/78068/2011), by Calouste Gulbenkian Foundation and by Fulbright Commission Portugal (grant ID 15122932). Célia M. Gouveia and Ricardo M. Trigo were supported by QSECA (PTDC/AAG-GLO/4155/2012). Steven W. Running was sponsored by the NASA MODIS Project (grant NNX11AF18G). The authors would like to thank Martin Wattenbach and the anonymous referees for the helpful comments.

Edited by: M. Reichstein

References

Ahlström, A., Miller, P. A., and Smith, B.: Too early to infer a global NPP decline since 2000, Geophys. Res. Lett., 39, L15403, doi:10.1029/2012GL052336, 2012.

Angert, A., Biraud, S., Bonfils, C., Henning, C. C., Buermann, W., Pinzon, J., Tucker, C. J., and Fung, I.: Drier summers cancel out the CO_2 uptake enhancement induced by warmer springs, P. Natl. Acad. Sci. USA, 102, 10823–10827, 2005.

Ballantyne, A. P., Alden, C. B., Miller, J. B., Tans, P. P., and White, J. W. C.: Increase in observed net carbon dioxide uptake by land and oceans during the past 50 years, Nature, 488, 70–72, 2012.

Balsamo, G., Beljaars, A., Scipal, K., Viterbo, P., van den Hurk, B., Hirschi, M., and Betts, A. K.: a Revised Hydrology for the ECMWF Model: Verification from Field Site to Terrestrial Water Storage and Impact in the Integrated Forecast System, J. Hydrometeorol., 10, 623–643, 2009.

Barriopedro, D., Fischer, E. M., Luterbacher, J., Trigo, R. M., and García-Herrera, R.: The Hot Summer of 2010: Redrawing the Temperature Record Map of Europe, Science, 332, 220–224, 2011.

Ciais, P., Reichstein, M., Viovy, N., Granier, A., Ogee, J., Allard, V., Aubinet, M., Buchmann, N., Bernhofer, C., Carrara, A., Chevallier, F., De Noblet, N., Friend, A. D., Friedlingstein, P., Grunwald, T., Heinesch, B., Keronen, P., Knohl, A., Krinner, G., Loustau, D., Manca, G., Matteucci, G., Miglietta, F., Ourcival, J. M., Papale, D., Pilegaard, K., Rambal, S., Seufert, G., Soussana, J. F., Sanz, M. J., Schulze, E. D., Vesala, T., and Valentini, R.: Europe-wide reduction in primary productivity caused by the heat and drought in 2003, Nature, 437, 529–533, 2005.

Coumou, D. and Rahmstorf, S.: a decade of weather extremes, Nature Clim. Change, 2, 491–496, http://dx.doi.org/10.1038/nclimate1452, 2012.

de Jong, R., Schaepman, M. E., Furrer, R., de Bruin, S., and Verburg, P. H.: Spatial relationship between climatologies and changes in global vegetation activity, Glob. Change Biol., 19, 1953–1964, 2013.

Dee, D. P., Uppala, S. M., Simmons, A. J., Berrisford, P., Poli, P., Kobayashi, S., Andrae, U., Balmaseda, M. A., Balsamo, G., Bauer, P., Bechtold, P., Beljaars, A. C. M., van de Berg, L., Bidlot, J., Bormann, N., Delsol, C., Dragani, R., Fuentes, M., Geer, A. J., Haimberger, L., Healy, S. B., Hersbach, H., Hólm, E. V., Isaksen, L., Kållberg, P., Köhler, M., Matricardi, M., McNally, A. P., Monge-Sanz, B. M., Morcrette, J.-J., Park, B.-K., Peubey, C., de Rosnay, P., Tavolato, C., Thépaut, J.-N., and Vitart, F.: The ERA-Interim reanalysis: configuration and performance of the data assimilation system, Q. J. Roy. Meteorol. Soc., 137, 553–597, 2011.

Ferranti, L. and Viterbo, P.: The European Summer of 2003: Sensitivity to Soil Water Initial Conditions, J. Climate, 19, 3659–3680, 2006.

Fischer, E. M. and Schär, C.: Consistent geographical patterns of changes in high-impact European heatwaves, Nat. Geosci., 3, 398–403, 2010.

Fischer, E. M., Seneviratne, S. I., Lüthi, D., and Schär, C.: Contribution of land-atmosphere coupling to recent European summer heat waves, Geophys. Res. Lett., 34, L06707, doi:10.1029/2006GL029068, 2007.

Frazier, A. E., Renschler, C. S., and Miles, S. B.: Evaluating post-disaster ecosystem resilience using MODIS GPP data, Int. J. Appl. Earth Obs., 21, 43–52, 2013.

Friedlingstein, P. and Prentice, I.: Carbon-climate feedbacks: a review of model and observation based estimates, Curr. Opin. Environ. Sust., 2, 251–257, 2010.

García-Herrera, R., Díaz, J., Trigo, R. M., Luterbacher, J., and Fischer, E. M.: a Review of the European Summer Heat Wave of 2003, Crit. Rev. Env. Sci. Tec., 40, 267–306, 2010.

Gouveia, C., Trigo, R. M., DaCamara, C. C., Libonati, R., and Pereira, J. M. C.: The North Atlantic Oscillation and European vegetation dynamics, Int. J. Climatol., 28, 1835–1847, 2008.

Hasenauer, H., Petritsch, R., Zhao, M., Boisvenue, C., and Running, S. W.: Reconciling satellite with ground data to estimate forest productivity at national scales, Forest Ecol. Manag., 276, 196–208, 2012.

Heimann, M. and Reichstein, M.: Terrestrial ecosystem carbon dynamics and climate feedbacks, Nature, 451, 289–292, 2008.

Hirschi, M., Seneviratne, S. I., Alexandrov, V., Boberg, F., Boroneant, C., Christensen, O. B., Formayer, H., Orlowsky, B., and Stepanek, P.: Observational evidence for soil-moisture impact on hot extremes in southeastern Europe, Nat. Geosci., 4, 17–21, 2011.

Janssens, I. A., Freibauer, A., Ciais, P., Smith, P., Nabuurs, G.-J., Folberth, G., Schlamadinger, B., Hutjes, R. W. A., Ceulemans, R., Schulze, E.-D., Valentini, R., and Dolman, A. J.: Europe's Terrestrial Biosphere Absorbs 7 to 12% of European Anthropogenic CO_2 Emissions, Science, 300, 1538–1542, 2003.

Jentsch, A., Kreyling, J., Elmer, M., Gellesch, E., Glaser, B., Grant, K., Hein, R., Lara, M., Mirzae, H., Nadler, S. E., Nagy, L., Otieno, D., Pritsch, K., Rascher, U., Schädler, M., Schloter, M., Singh, B. K., Stadler, J., Walter, J., Wellstein, C., Wöllecke, J., and Beierkuhnlein, C.: Climate extremes initiate ecosystem-regulating functions while maintaining productivity, J. Ecol., 99, 689–702, 2011.

Kreyling, J., Wenigmann, M., Beierkuhnlein, C., and Jentsch, A.: Effects of Extreme Weather Events on Plant Productivity and Tissue Die-Back are Modified by Community Composition, Ecosystems, 11, 752–763, 2008.

Le Quéré, C., Raupach, M. R., Canadell, J. G., and Marland et al., G.: Trends in the sources and sinks of carbon dioxide, Nat. Geosci., 2, 831–836, doi:10.1038/ngeo689, 2009.

Luterbacher, J., Dietrich, D., Xoplaki, E., Grosjean, M., and Wanner, H.: European Seasonal and Annual Temperature Variability, Trends, and Extremes Since 1500, Science, 303, 1499–1503, 2004.

Medlyn, B. E.: Comment on "Drought-Induced Reduction in Global Terrestrial Net Primary Production from 2000 Through 2009", Science, 333, 1093, doi:10.1126/science.1199544, 2011.

Meehl, G. A. and Tebaldi, C.: More Intense, More Frequent, and Longer Lasting Heat Waves in the 21st Century, Science, 305, 994–997, 2004.

Meir, P., Cox, P., and Grace, J.: The influence of terrestrial ecosystems on climate, Trends Ecol. Evol., 21, 254–260, 2006.

Menzel, A., Sparks, T. H., Estrella, N., Koch, E., Aasa, A., Ahas, R., Alm-Kobler, K., Bissolli, P., Braslavska, O., Briede, A., Chmielewski, F. M., Crepinsek, Z., Curnel, Y., Dahl, A., Defila, C., Donnelly, A., Filella, Y., Jatczak, K., Mage, F., Mestre, A., Nordli, O., Penuelas, J., Pirinen, P., Remisova, V., Scheifinger, H., Striz, M., Susnik, a., Van Vliet, A. J. H., Wielgolaski, F.-E., Zach, S., and Zust, A.: European phenological response to climate change matches the warming pattern, Glob. Change Biol., 12, 1969–1976, 2006.

Mu, Q., Heinsch, F. A., Zhao, M., and Running, S. W.: Development of a global evapotranspiration algorithm based on MODIS and global meteorology data, Remote Sens. Environ., 111, 519–536, 2007.

Myneni, R., Hoffman, S., Knyazikhin, Y., Privette, J., Glassy, J., Tian, Y., Wang, Y., Song, X., Zhang, Y., Smith, G., Lotsch, A., Friedl, M., Morisette, J., Votava, P., Nemani, R., and Running, S.: Global products of vegetation leaf area and fraction absorbed PAR from year one of MODIS data, Remote Sens. Environ., 83, 214–231, 2002.

Nemani, R. R., Keeling, C. D., Hashimoto, H., Jolly, W. M., Piper, S. C., Tucker, C. J., Myneni, R. B., and Running, S. W.: Climate-Driven Increases in Global Terrestrial Net Primary Production from 1982 to 1999, Science, 300, 1560–1563, 2003.

Pan, Y., Birdsey, R. A., Fang, J., Houghton, R., Kauppi, P. E., Kurz, W. A., Phillips, O. L., Shvidenko, A., Lewis, S. L., Canadell, J. G., Ciais, P., Jackson, R. B., Pacala, S. W., McGuire, A. D., Piao, S., Rautiainen, A., Sitch, S., and Hayes, D.: a Large and Persistent Carbon Sink in the World's Forests, Science, 333, 988–993, 2011.

Peng, S., Piao, S., Ciais, P., Myneni, R. B., Chen, A., Chevallier, F., Dolman, A. J., Janssens, I. A., Penuelas, J., Zhang, G., Vicca, S., Wan, S., Wang, S., and Zeng, H.: Asymmetric effects of daytime and night-time warming on Northern Hemisphere vegetation, Nature, 501, 88–92, doi:10.1038/nature12434, 2013.

Piao, S., Ciais, P., Friedlingstein, P., Peylin, P., Reichstein, M., Luyssaert, S., Margolis, H., Fang, J., Barr, A., Chen, A., Grelle,

A., Hollinger, D. Y., Laurila, T., Lindroth, A., Richardson, A. D., and Vesala, T.: Net carbon dioxide losses of northern ecosystems in response to autumn warming, Nature, 451, 49–52, doi:10.1038/nature06444, 2008.

Reichstein, M., Ciais, P., Papale, D., Valentini, R., Running, S., Viovy, N., Cramer, W., Granier, A., Ogée, J., Allard, V., Aubinet, M., Bernhofer, C., Buchmann, N., Carrara, A., Gronwald, T., Heimann, M., Heinesch, B., Knohl, A., Kutsch, W., Loustau, D., Manca, G., Matteucci, G., Miglietta, F., Ourcival, J., Pilegaard, K., Pumpanen, J., Rambal, S., Schaphoff, S., Seufert, G., Soussana, J.-F., Sanz, M.-J., Vesala, T., and Zhao, M.: Reduction of ecosystem productivity and respiration during the European summer 2003 climate anomaly: a joint flux tower, remote sensing and modelling analysis, Glob. Change Biol., 13, 634–651, 2007.

Reichstein, M., Bahn, M., Ciais, P., Frank, D., Mahecha, M. D., Seneviratne, S. I., Zscheischler, J., Beer, C., Buchmann, N., Frank, D. C., Papale, D., Rammig, A., Smith, P., Thonicke, K., van der Velde, M., Vicca, S., Walz, A., and Wattenbach, M.: Climate extremes and the carbon cycle, Nature, 500, 287–295, doi:10.1038/nature12350, 2013.

Roy, D., Jin, Y., Lewis, P., and Justice, C.: Prototyping a global algorithm for systematic fire-affected area mapping using MODIS time series data, Remote Sens. Environ., 97, 137–162, 2005.

Rudolf, B. and Schneider, U.: Calculation of Gridded Precipitation Data for the Global Land-Surface using in-situ Gauge Observations, vol. Proceedings of the 2nd Workshop of the International Precipitation Working Group IPWG,Monterey October 2004, 231–247, EUMETSAT, iSBN 92-9110-070-6, ISSN 1727-432X, 2005.

Running, S. W., Nemani, R. R., Heinsch, F. A., Zhao, M., Reeves, M., and Hashimoto, H.: a Continuous Satellite-Derived Measure of Global Terrestrial Primary Production, BioScience, 54, 547–560, 2004.

Schär, C., Vidale, P. L., Luthi, D., Frei, C., Haberli, C., Liniger, M. A., and Appenzeller, C.: The role of increasing temperature variability in European summer heatwaves, Nature, 427, 332–336, 2004.

Schubert, P., Lagergren, F., Aurela, M., Christensen, T., Grelle, A., Heliasz, M., Klemedtsson, L., Lindroth, A., Pilegaard, K., Vesala, T., and Eklundh, L.: Modeling GPP in the Nordic forest landscape with MODIS time series data - Comparison with the MODIS GPP product, Remote Sens. Environ., 126, 136–147, 2012.

Schwalm, C. R., Williams, C. A., Schaefer, K., Baldocchi, D., Black, T. A., Goldstein, A. H., Law, B. E., Oechel, W. C., Paw U, K. T., and Scott, R. L.: Reduction in carbon uptake during turn of the century drought in western North America, Nat. Geosci., 5, 551–556, 2012.

Seneviratne, S. I., Luthi, D., Litschi, M., and Schar, C.: Land-atmosphere coupling and climate change in Europe, Nature, 443, 205–209, 2006.

Smith, M. D.: An ecological perspective on extreme climatic events: a synthetic definition and framework to guide future research, J. Ecol., 99, 656–663, 2011.

Teuling, A. J., Seneviratne, S. I., Stockli, R., Reichstein, M., Moors, E., Ciais, P., Luyssaert, S., van den Hurk, B., Ammann, C., Bernhofer, C., Dellwik, E., Gianelle, D., Gielen, B., Grunwald, T., Klumpp, K., Montagnani, L., Moureaux, C., Sottocornola, M., and Wohlfahrt, G.: Contrasting response of European forest and grassland energy exchange to heatwaves, Nat. Geosci., 3, 722–727, 2010.

Trigo, R. M., García-Herrera, R., Díaz, J., Trigo, I. F., and Valente, M. A.: How exceptional was the early August 2003 heatwave in France?, Geophys. Res. Lett., 32, L10701, doi:10.1029/2005GL022410, 2005.

Zhao, M. and Running, S. W.: Drought-Induced Reduction in Global Terrestrial Net Primary Production from 2000 Through 2009, Science, 329, 940–943, 2010.

Zhao, M. and Running, S. W.: Response to Comments on Drought-Induced Reduction in Global Terrestrial Net Primary Production from 2000 Through 2009, Science, 333, 1093, doi:10.1126/science.1199169, 2011.

Zhao, M., Heinsch, F. A., Nemani, R. R., and Running, S. W.: Improvements of the MODIS terrestrial gross and net primary production global data set, Remote Sens. Environ., 95, 164–176, 2005.

Zhao, M., Running, S. W., and Nemani, R. R.: Sensitivity of Moderate Resolution Imaging Spectroradiometer (MODIS) terrestrial primary production to the accuracy of meteorological reanalyses, J. Geophys. Res.-Biogeo., 111, G01002, doi:10.1029/2004JG000004, 2006.

Zhou, L., Tucker, C. J., Kaufmann, R. K., Slayback, D., Shabanov, N. V., and Myneni, R. B.: Variations in northern vegetation activity inferred from satellite data of vegetation index during 1981 to 1999, J. Geophys. Res., 106, 20069–20083, 2001.

Zscheischler, J., Mahecha, M. D., Harmeling, S., and Reichstein, M.: Detection and attribution of large spatiotemporal extreme events in Earth observation data, Ecol. Inform., 15, 66–73, 2013.